

1 **Electron Paramagnetic Resonance spin trapping of sunflower and olive oils**  
2 **subjected to thermal treatment: optimization of experimental and fitting**  
3 **parameters.**

4

5

6 Angela Fadda<sup>a,\*</sup>, Maria Giovanna Molinu<sup>a</sup>, Pierfrancesco Deiana<sup>c</sup>, Daniele Sanna<sup>b,\*</sup>

7

8

9 <sup>a</sup> Istituto di Scienze delle Produzioni Alimentari, Consiglio Nazionale delle Ricerche, Traversa la Crucca 3, I-  
10 07100 Sassari, Italy

11 <sup>b</sup> Istituto di Chimica Biomolecolare, Consiglio Nazionale delle Ricerche, Traversa La Crucca 3, I-07100Sassari,  
12 Italy

13 <sup>c</sup> Dipartimento di Agraria, Università degli Studi di Sassari, viale Italia 39, I-07100 Sassari, Italy.

14 \* corresponding authors: Angela Fadda, [angela.fadda@cnr.it](mailto:angela.fadda@cnr.it); Daniele Sanna, [daniele.sanna@cnr.it](mailto:daniele.sanna@cnr.it);

15

16

17 **Abstract**

18 Sunflower oil (SO) and extra virgin olive oil (EVOO) were heated at 90 °C in the presence of PBN. The radical  
19 species formed during thermal treatment, trapped by PBN, were revealed by Electron Paramagnetic  
20 Resonance (EPR) spectroscopy, a widely used method to study oils' oxidation.

21 The effect of the experimental parameters on the intensity of PBN adduct was analyzed with the aim to  
22 standardize the spin trapping protocol for oils. A modification of the Boltzmann sigmoidal equation was  
23 proposed to fit the experimental points representing the changes of the EPR intensity of the PBN adduct vs.  
24 time. The fitting parameters allowed for distinguishing between SO and EVOO and to obtain more reliable  
25 Induction Period (IP) values. The fitting parameters and the shape of the curve depend on the diameter of  
26 the sample holder. The IP and the time at which maximum intensity is reached,  $t(I_{max})$ , in thin capillary  
27 tubes (IP 35.92 min,  $t(I_{max})$  186 min) were shifted at longer times in comparison with flat cell (IP 69.54 min,  
28  $t(I_{max})$  106 min). The peroxide values (PV) were measured in SO and EVOO samples, with and without PBN,  
29 at specific points of the curve and related to the intensity of the EPR signals. PBN inhibits the propagation  
30 of the chain reaction and the extent of inhibition is lower in EVOO than in SO maybe due to the effect of  
31 phenolic compounds that in SO are lacking. The phenolic compounds are also the responsible for the lower  
32 PBN adduct intensities observed in EVOO than in SO. This study further highlights the power of EPR  
33 spectroscopy in the evaluation of oil oxidation and provides a guide for EPR experimental and fitting  
34 parameters for oils.

35

36

37 **Keywords:**-Electron Paramagnetic Resonance (EPR), *N-tert-butyl- $\alpha$ -phenylnitron* (PBN), 5,5-dymethyl-1-  
38 pyrroline N-oxide (DMPO), spin trapping, Extra Virgin Olive Oil, sunflower oil.

39

## 40 INTRODUCTION

41 Oil oxidation, triggered by oxygen, light, and metals, is an important challenge for food industries.  
42 Byproducts produced during oil oxidation can reduce the nutritional quality of food and may be harmful to  
43 human health. In oils, lipid oxidation is a chain reaction that involves three steps: initiation, propagation,  
44 and termination.<sup>1-3</sup> Hydroperoxides are the primary oxidation products. At room temperature, they are  
45 relatively stable; however, at high temperatures they rapidly decompose to alkoxy radicals, which, due to  
46 the homolytic  $\beta$ -scission of the carbon-carbon bond, form alkyl radicals.<sup>2</sup> The extent of oil oxidation  
47 depends on oil fatty acid composition, the presence of antioxidants, and external factors like temperature  
48 and oxygen.<sup>2</sup>

49 The methods used to study the oil oxidation processes and to assess the oxidation status of oils are based  
50 on the analysis of primary or secondary oxidation products. Peroxide value (PV), P-anisidine value (AV), the  
51 ThioBarbituric Acid Reactive Substances (TBARS), conjugated dienes, and trienes are the most frequently  
52 used. Together with these methods, other methodologies have been developed to analyze, on different  
53 oils, the oxidation process. The EPR spectroscopy coupled with the spin trapping method has been  
54 employed to study the thermo-induced oxidation processes of plant extracts, alcoholic beverages, food  
55 lipids, bulk oils, and oil emulsions.<sup>4-7</sup> Peroxyl and alkoxy radicals formed during oil oxidation are trapped by  
56 *N-tert-butyl- $\alpha$ -phenylnitrone* (PBN), the most widely used open-chain nitron spin trap, forming a PBN  
57 radical adduct, that being relatively stable is easily detected by EPR. The EPR spin trapping technique has  
58 been applied to olive, peanut, rapeseed, soybean, sunflower, and fish oils to study oils' oxidative stability  
59 and correlate it with oils' shelf life.<sup>4, 8-12</sup> In these papers the oxidative stability experiments were carried out  
60 by subjecting oils to mild thermal treatments, with temperatures not higher than 70 °C, heating the oils  
61 outside the EPR cavity, then measuring the adduct intensity at room temperature.<sup>4, 8-12</sup> The oxidative  
62 stability is measured as induction period (IP), defined as the time at which the radical adducts increase  
63 suddenly after a slow increase of their concentration. The IP is calculated by a bilinear regression that  
64 involves the points with a low PBN adduct intensity and those with a sharp increase of the adduct signal.  
65 The drawback is that this calculation is rather subjective and may provide different results.

66 Other authors investigated, by EPR spectroscopy, the evolution of lipid oxidation products of bulk oils and  
67 fatty acids methyl esters during controlled thermal treatments at different temperatures.<sup>13-15</sup> In a kinetic  
68 study of the oxidation products of peanut oil treated at 180 °C, Silvagni *et al.*<sup>13</sup> followed the formation of  
69 PBN adducts for 40 minutes and determined the contribution of the identified radical species for each point  
70 of the kinetic curve. On grape seed oil and on fatty acids methyl esters, some authors described, with the  
71 EPR spin trapping technique, the formation and the decomposition of the radical adducts produced during  
72 oils thermal treatment at 105 °C.<sup>14, 15</sup> More recently on peanut oil Jiang *et al.*,<sup>11</sup> followed by EPR the  
73 formation of PBN radical adducts at different temperatures (60, 80, 90 °C) with the aim to identify the IP  
74 value with the Boltzmann sigmoidal equation according to Barr *et al.*<sup>16</sup> In these experiments the changes of

75 intensity of the PBN-adduct over the time were generally studied for short periods. Even when the  
76 formation and decomposition of the radical adducts were studied for a longer period of time, no fitting of  
77 the experimental points was provided.

78 The role of oxygen in oils' oxidation has been widely studied;<sup>3</sup> at temperatures lower than 60 °C the  
79 amount of oxygen dissolved depends on oil's composition and on the oxygen partial pressure above oil  
80 surface. By contrast at temperature higher than 60 °C the amount of oxygen dissolved decreases with  
81 increasing temperatures. In this context the headspace oxygen becomes the supply for reaction with lipids.<sup>3</sup>  
82 In EPR experiments, aimed at determining oils shelf life or monitoring the amount of radicals in oils  
83 subjected to thermal treatment, the effects of the exposed surface of oil in the sample holder on the  
84 changes of intensity of PBN-adduct have never been taken into consideration. As a matter of fact, in papers  
85 dealing with the effects of thermal treatments on oil oxidation, authors generically indicated that  
86 experiments were performed in EPR tubes, which usually have an internal diameter of 3 or 4 mm<sup>11, 17</sup> or in  
87 capillary tubes<sup>5</sup>.

88 In this paper, we followed by EPR spin trapping technique the evolution of PBN adducts over time in SO and  
89 EVOO subjected to thermal treatments at 90 °C. The aim is to describe the evolution pattern of the PBN  
90 adduct and to fit it with mathematical functions characterized by parameters that distinguish between SO  
91 and EVOO and to easily identify the IP value. For this purpose, a modification of the Boltzmann sigmoidal  
92 equation is proposed to improve the fitting of the curve and to give more reliable IP values.

93 Moreover, with the aim to standardize the spin trapping protocol for oils, the effect on the kinetic curve of  
94 the shape of the sample holder, where the experiments were performed, has been investigated.

95 Finally, the peroxide values have been measured in thermally treated samples with and without PBN, and  
96 these values have been related to the PBN signal intensity.

97

## 98 **MATERIALS AND METHODS**

### 99 **Materials**

100 Hydroxytyrosol ( $\geq 98\%$ ) and tyrosol ( $\geq 98\%$ ), oleuropein ( $\geq 98\%$ ), vanillin ( $\geq 99\%$ ), vanillic acid ( $\geq 97\%$ ), p-  
101 coumaric acid ( $\geq 98\%$ ), pinoresinol ( $\geq 95\%$ ), luteolin ( $\geq 98\%$ ), apigenin ( $\geq 95\%$ ) methanol for HPLC ( $\geq 99.9\%$ ),  
102 ethanol, PBN (*N-tert-butyl- $\alpha$ -phenylnitrone*), isooctane and ammonium thiocyanate were purchased from  
103 Sigma-Aldrich (Milan, Italy), and acetonitrile by ChemLab (Zedelgen, Belgium). DMPO (5,5-dimethyl-1-  
104 pyrroline N-oxide) was purchased from Enzo Life and used without further purification. Ultrapure water  
105 was prepared using a Milli-Q system (Millipore Corporation, Billerica, MA, USA).

106 SO was purchased from the local market, while EVOO was obtained from a local producer. Upon arrival at  
107 the laboratory, oils were stored at  $-20$  °C until analysis.

108

### 109 **Identification and quantification of phenolic compounds**

110 The profile and the concentration of phenolic compounds were analyzed in SO and EVOO. Phenolic  
111 compounds were extracted according to Deiana *et al.*<sup>18</sup> mixing 4 g of oil sample with 5 ml of  
112 methanol/water (8:2, v/v). The mixture was shaken (30 min) and centrifuged at 5000 rpm (15 min), then  
113 the polar supernatant was separated and analyzed to determine the concentration of phenols. The  
114 extraction process was performed twice and the extracted polar fraction filtered through 0.45  $\mu\text{m}$  PVDV  
115 filters. The separation and quantification of phenolic compounds were performed by HPLC using an Agilent  
116 1100 system (Agilent Technologies, Palo Alto, CA, USA) equipped with a quaternary pump (G1311A), a  
117 degasser, column thermostat, an auto-sampler (G1313A), and a diode array detector (G1315 B, DAD). A C-  
118 18 Luna column (250 x 4.6 mm, 5  $\mu\text{m}$ ; Phenomenex, Torrance, CA, USA) with a security guard cartridge (4 x  
119 2 mm) was used for chromatographic separation. The flow rate was set at 1 mL/min, column temperature  
120 30 °C, injection volume was 20  $\mu\text{L}$ . Phenolic compounds were quantified based on their respective standard  
121 ( $\text{mg L}^{-1}$ ), whereas secoiridoids and 1-acetoxypinoresinol were quantified using oleuropein and pinoresinol  
122 as standards. Results were expressed as mg of phenolic compounds  $\text{kg}^{-1}$  of oil.

123

#### 124 **Thermal treatment and EPR spin trapping analysis of SO and EVOO**

125 EPR measurements were carried out with a Bruker EMX spectrometer operating at the X-band (9.4 GHz)  
126 equipped with an HP 53150A frequency counter and a variable temperature unit ER 4111 VT. Spectra were  
127 acquired with Bruker WinEPR Acquisition Version 4.33 and simulated with Bruker WINEPR SimFonia Version  
128 1.26.

129 SO and EVOO containing the spin trap PBN were heated at 90 °C inside the EPR cavity.

130 Five  $\mu\text{L}$  of a 2.5 M PBN solution in absolute ethanol were dried under a nitrogen flow to avoid any  
131 interference of ethanol during spin trapping experiment. Hundred  $\mu\text{L}$  of oil were mixed with the solid PBN.  
132 To evaluate the effect of the shape of the sample holder on the kinetic of the PBN adduct formation, a flat  
133 cell and two capillary tubes differing for the diameter of the capillary were tested. The flat cell was a  
134 cylindrical quartz tube with an inner diameter of 2.5 mm (exposed oil surface 5  $\text{mm}^2$ ) with a 25 mm  
135 terminal flat part at the bottom. The large capillary tubes had a diameter of 1.6 mm and an exposed oil  
136 surface of 2  $\text{mm}^2$ , whereas the thin capillary tubes had a diameter of 1.1 mm and an oil exposed surface of  
137 1  $\text{mm}^2$ . In each sample holder, 100  $\mu\text{L}$  of oil with PBN were transferred.

138 EPR spectra were acquired every 5 minutes for 5 hours. The EPR instrument was set under the following  
139 conditions: modulation frequency 100 kHz, modulation amplitude 0.106 mT, receiver gain 5 x 10<sup>4</sup>,  
140 microwave power 20 mW (which is with the ER 4119HS cavity, below the saturation limit), resolution 1024  
141 points, sweep time 167.772 s, time constant and conversion time 163.84 msec. The selected values of time  
142 constant, sweep time, resolution, and sweep width allow to resolve the narrowest line corresponding to  
143 0.049 mT. These parameters were optimized with preliminary analysis on different oils.

144 The intensity of the PBN-adduct was estimated from the double integration of the spectra and was plotted  
145 against time.

146 The experimental points followed a double sigmoidal growth and decrease pattern. The first part of the  
147 curve, from the beginning of the experiment to the achievement of the maximum intensity, was fitted with  
148 a modified Boltzmann sigmoid equation. The modified equation, proposed here for the first time, is the  
149 following:

150

$$151 \quad Y = \text{Bottom} + (\text{Top} - \text{Bottom}) / (1 + \exp(V_{50} - x) / \text{slope}) + \text{rise} * x$$

152 The second part of the curve that includes the points from the maximum of intensity to the end of the  
153 experiment was fitted with a reverse Boltzmann modified sigmoid equation:

154

$$155 \quad Y = (((\text{Top} - \text{Final}) / (1 + \exp(x - \text{Mid}_2) / \text{slope})) + \text{Final}) - \text{decline} * x$$

156

157 The experimental points were fitted with GraphPad Prism8 for Windows software (GraphPad Software Inc.  
158 La Jolla, CA92037, USA).

159

#### 160 **DMPO spin trapping experiments**

161 100  $\mu\text{L}$  of a DMPO solution (0.125 mM) in absolute ethanol were dried under a nitrogen flow. One hundred  
162  $\mu\text{L}$  of SO were mixed with the spin trap, placed in a flat cell, and inserted into the EPR cavity heated at 90  
163  $^{\circ}\text{C}$ . EPR spectra were acquired every 5 minutes for 4 hours.

164

#### 165 **Effect of PBN and oxygen availability on lipid oxidation**

166 To draw a more complete picture of the reactions taking place during oil's thermal treatment and to  
167 evaluate the effect of PBN on lipid oxidation, SO and EVOO were heated in a thermostatic bath set at 90  $^{\circ}\text{C}$ .  
168 One hundred and fifty  $\mu\text{L}$  of oil with and without PBN were placed in 1.5 ml safe-lock tubes. For samples  
169 with PBN, aliquots of 7.5  $\mu\text{L}$  of a 2.5 M PBN solution in absolute ethanol were dried under a nitrogen flow  
170 and mixed with the oil. At fixed time intervals, oil samples were analyzed for the concentration of  
171 peroxides, spectrophotometric constants, and PBN adduct concentration. SO and EVOO were heated for 30  
172 h. For sunflower oil, samples were taken at 0.5, 1, 2, 3, 4, 6, 12, 15, 20 and 30 hours, whereas for olive oil  
173 they were withdrawn at 6, 12, 15, 20, and 30 hours.

174 To evaluate the effects of oxygen availability and oil surface exposed to air (S) on peroxide values and on  
175 PBN adduct intensity, SO was placed in 1.5 mL or 0.5 mL sample tubes, with or without PBN (final  
176 concentration 125 mM). Tubes of 1.5 mL capacity and an air-exposed surface of 33.18  $\text{mm}^2$  were filled with  
177 200  $\mu\text{L}$  of oil, whereas 0.5 mL tubes with an air-exposed surface of 25.50  $\text{mm}^2$  were filled with 150  $\mu\text{L}$  of oil.

178 In half of the sample tubes (both 1.5 and 0.5 mL), the headspace volume has been reduced by inserting a  
179 small metal cylinder to limit oxygen availability. All tubes were heated at 90 °C for 15 hours.

180

### 181 **Spectrophotometric detection of peroxide value and conjugated dienes**

182 Peroxides were determined according to the International Dairy Federation method described by Shantha  
183 *et al.*<sup>19</sup> The method is based on the oxidation of Fe(II) to Fe(III) by hydro-peroxides and on the formation of  
184 a red Fe(III)-thiocyanate complex. Briefly, about 10 mg of EVOO or SO were mixed with 9.8 mL of  
185 chloroform-methanol 7:3 (v/v) and vortexed. Fifty  $\mu\text{L}$  of ammonium thiocyanate solution (394 mM, 30 g in  
186 100 ml of  $\text{H}_2\text{O}$ ) were added to the mixture, vortexed, then 50  $\mu\text{L}$  of a  $\text{FeSO}_4 \cdot 7\text{H}_2\text{O}$  (18 mM, 30 g in 100 ml of  
187  $\text{H}_2\text{O}$  containing 2 ml of HCl 10 M) were mixed. After 15 minutes, the absorbance was measured at 507 nm  
188 with a Perkin-Elmer Lambda 35 spectrophotometer. Peroxide value was expressed as micro-equivalents of  
189 peroxides  $\cdot \text{g}^{-1}$  of oil, based on a calibration curve built using  $\text{FeCl}_3 \cdot 6\text{H}_2\text{O}$  as Fe(III) source (Fe(III):  $6.1 \times 10^{-5}$  –  
190  $4.6 \times 10^{-4}$  M;  $R^2 = 0.99$ ).

191 Peroxide values were also determined in SO containing PBN at the final concentrations of 62.5, 125, and  
192 250 mM. Sample tubes (1.5 mL capacity) containing 100  $\mu\text{L}$  of SO and PBN were heated at 90 °C for 5 hours  
193 (300 min), then the peroxide value was determined

194 Conjugated dienes and trienes absorb in the ultraviolet region of the spectrum and are frequently used to  
195 determine the oils spectroscopic index (K232 and K268). The spectroscopic index was assessed according to  
196 the method proposed by the International Olive Oil Council.<sup>20</sup> Samples were prepared using 1% w/v  
197 solutions of the oils in isooctane. The specific absorbance values at 232 and 268 nm were recorded with an  
198 Agilent spectrophotometer (8453 UV-Visible Spectrophotometer, Agilent Technologies, Palo Alto, CA, USA)  
199 against a blank of pure isooctane in 1 cm optical path-length UV-cuvettes. Since PBN absorbs in the  
200 ultraviolet region of the spectrum, the absorbance of samples containing PBN was corrected for the  
201 absorbance of an equimolar PBN solution in isooctane.

202

### 203 **Statistical analysis**

204 Statistical analysis was performed with GraphPad Prism8 for Windows software (GraphPad Software Inc. La  
205 Jolla. CA92037, USA). A one-way ANOVA was used to compare the results of peroxides, conjugated dienes,  
206 and kinetic parameters calculated from sunflower and olive oils kinetic curves. Three replications were  
207 performed for each analysis. In addition, means separation was calculated by Tukey's test or t-test at  $P \leq$   
208 0.05.

209

210

## 211 **RESULTS**

### 212 **Oil phenolic composition**

213 EVOO is rich in phenolic compounds (Table S1), as expected, in the SO no phenolic compounds were  
214 detected. Oleocanthal (p-HPEA-EDA), oleacin (3,4-DHPEA-EDA), and the aglyconic derivatives of oleuropein  
215 (3,4-DHPEA-EA) and ligstroside (p-HPEA-EA) represent over 90% of the total phenols detected in olive oils.  
216 These compounds own antioxidant properties and are responsible for EVOO health properties.<sup>21</sup> Other  
217 phenolic compounds such as hydroxytyrosol (3,4-DHPEA), tyrosol (p-HPEA), 1-acetoxypinoresinol, vanillin,  
218 phenolic acids (*o*- and *p*-coumaric and vanillic acid), and flavonoids (luteolin and apigenin) are also present.  
219

## 220 **Thermal treatment of sunflower oil at 90 °C with PBN and DMPO**

221 PBN (*t*-butyl- $\alpha$ -phenyl nitron) is by far the most frequently employed open-chain nitron spin trap. It is  
222 used to trap 1-hydroxyethyl radicals in wines, beer, or ethanolic plant extracts and lipid-derived radicals in  
223 oils.<sup>7, 22-24</sup> Figure 1A shows the EPR spectra of PBN adduct generated during the thermal treatment of  
224 sunflower oil at 90 °C. When different radical species are contemporaneously present and trapped by PBN,  
225 their identification is not easy because the variation of the spectroscopic parameters of the spin adducts is  
226 little.

227 The only observable coupling constant, besides that of the nitrogen itself, is that with the  $\beta$  hydrogen.  
228 These two coupling constants vary in a small range  $a_N$  1.415 – 1.496 mT and  $a_H$  0.210 – 0.375 mT for  
229 alkyl/alkoxyl radical adducts. Moreover, there is no any evident trend in relation to the trapped radical.<sup>25</sup>  
230 Yamada *et al.*<sup>26</sup> reported the  $a_N$  and  $a_H$  values of 13.44 and 1.63 G for the adducts of peroxy radical of  
231 methyl linoleate; for the corresponding alkoxyl radical, the values were 14.22 and 2.10 G, and finally, for  
232 the carbon-centered radical, the values were 15.03 and 2.83 G.

233

234 Figure 1

235

236 During the thermal treatment of sunflower oil at 90 °C in the flat cell, three different spectra are  
237 distinguishable, although their hyperfine constants vary very little (Figure 1A). The first spectrum (black line  
238 in Figure 1) obtained after 36 min has been satisfactorily simulated with  $a_N$  1.488 mT,  $a_H$  0.205 mT, and  $g$   
239 2.00610; the second one (in red line Figure 1A), obtained after 106 min, has  $a_N$  1.494 mT,  $a_H$  0.210 mT and  $g$   
240 2.00614; finally, the species present after 146 min (in blue in Figure 1A) is characterized by  $a_N$  1.490 mT,  $a_H$   
241 0.215 mT and  $g$  2.00617. The selected time intervals correspond approximately to the lag time (36 min), to  
242 the time at which the maximum EPR intensity was reached (106 min), and to the final time (146 min), see  
243 Figure 2 and Table 2. Thus, the parameters of these three species are very similar, but, as we previously  
244 mentioned, it very hard to distinguish between the various types of adducts based on these variations.



245 At the beginning of the experiments performed with PBN, a species with  $a_N$  1.4950 mT,  $a_H$  0.4900 mT, and  $g$   
246 2.00555 has been identified (see Figure S2); this species could be an adduct of MNP (2-methyl-2-  
247 nitrosopropane) derived from the decomposition of the PBN-OOR adduct, as reported in the literature.<sup>5, 15</sup>  
248 Vicente *et al.*,<sup>15</sup> in the thermal treatment at 105 °C of fatty acids methyl esters, detected three adducts:  
249 peroxy and alkyl adducts of PBN and one of MNP, a degradation product of PBN. The importance of  
250 peroxy adduct was more significant than the other adducts at lower temperatures, while the alkyl adduct  
251 increased its concentration when oxygen was lacking.

252 To identify the radical species produced, the sunflower oil was heated at 90 °C in the presence of DMPO  
253 instead of PBN. With the cyclic spin trap DMPO (5,5-dimethyl-1-pyrroline *N*-oxide), the variation of the  
254 splitting due to the  $\beta$  hydrogens is much larger and depends on the nature of the trapped radical being  $\geq 20$   
255 G for the alkyl radicals and between 0.6 and 0.8 mT for the alkoxy radicals.

256 Unlike the adducts with the PBN, those with the DMPO give more information on the nature of the trapped  
257 radical. However, there are two problems connected with the use of this spin trap: i) the first is that PBN has more  
258 frequently been used in the literature studies of oils; ii) the second is that the adducts formed with DMPO are less  
259 stable in comparison with those of PBN and in fact, the intensity of the EPR signals in the first case is much lower. In  
260 agreement with our results, Xie *et al.*<sup>17</sup> showed that it is more easy with DMPO, in comparison with PBN, to distinguish  
261 between different types of adduct formed by peroxy, alkoxy and alkyl radicals formed during the thermal treatment  
262 at 90 °C of oleic and linoleic acids. Two main adducts can be identified (see Figure 1B).

263 These DMPO-adducts were simulated with the following parameters:  $a_N$  1.4876 mT,  $a_H$  0.2081 mT and  $a_N$   
264 1.425 mT,  $a_H$  2.010 mT while  $g$  2.0078 for both (see Figure 1Bb).

265 The DMPO-adduct with  $a_H$  2.01 mT can be identified as an alkyl adduct, probably formed after the  
266 displacement of the allylic hydrogen on the carbon adjacent to one (or two) double bond(s) of oleic (or  
267 linoleic) acid(s). Alberti and Macciantelli<sup>25</sup> identified a species with an  $a_H$  value in the range 6-8 G assigned  
268 to the trapping of an alkoxy radical. In our experiment, this species was not detected, but we identified a  
269 species with  $a_H$  0.2081 mT. Similarly, other authors<sup>17, 27</sup> observed, during the thermal oxidation of oleic acid,  
270 a DMPO adduct having  $a_H$  0.212 mT and 0.19921 mT, respectively, and interpreted this splitting as due to  
271 the  $\gamma$  hydrogen of an oxidized DMPO adduct where the  $\beta$  hydrogen was lost. Besides the species with  $a_H$   
272 0.2081 mT, we observed another species with only three lines. This species, more likely an oxidized DMPO  
273 adduct where the  $\beta$  hydrogen has been lost, increases its intensity up to 11 min, then decreases without  
274 disappearing and can be distinguished again at the end of the experiment ( $a_N$  1.400 mT,  $g$  2.00553, see  
275 Figure 1Ba).

276 Other minor adducts are present at the beginning of the experiment, but these quickly disappear and are  
277 difficult to be identified (see peaks indicated by \* in Figure 1Ba), similarly as observed with PBN.

278  
279

## 280 Kinetic analysis of PBN adduct

### 281 Sunflower oil thermal treatment: fitting of the kinetic curve

282 SO was used as a model to study the kinetic of PBN-adduct of oils subjected to thermal treatment at 90 °C.  
283 Figure S3 reports the EPR intensity of the PBN-adduct as a function of time. The resulting pattern can be  
284 associated with a double sigmoidal curve. This kinetic pattern described by Caglar *et al.*<sup>28</sup> is quite common  
285 in biological systems and can be considered as the sum of two phases: an exponential increase followed by  
286 a decay. In the oxidation process of sunflower oil, at  $t_0$  the beginning of the experiment, the intensity of the  
287 adduct is rather low and increases continuously until the intensity of the signal rises sharply. After the lag  
288 time, the intensity of the PBN-adduct increases exponentially until the achievement of a maximum beyond  
289 which a decay of the signal intensity is observed. On oil, the changes of PBN-adduct intensity over time  
290 were only partially studied without analyzing in detail the shape of the resulting curve<sup>13</sup>. On wine, the  
291 changes of the 1-hydroxyethyl radical (HER) –POBN adduct over time were followed from the beginning of  
292 the experiment to achieving the maximum adduct intensity. Wines were classified according to the  
293 parameters extracted from the experimental curve:  $I_{\max}$  (the maximum intensity of the adduct) and  $r_{\text{POBN-HER}}$   
294 (the rate of increase of the adduct).<sup>24</sup> Similarly, on soybean oil, the PBN-adduct signal growth was  
295 suggested as a tool to measure oil rancidity.<sup>16</sup>

296 The kinetic pattern of the PBN spin trap adduct described in this paper for SO is similar to that described by  
297 Samouilov *et al.*<sup>29</sup> for DEPMPPO-OOH adduct (5-diethoxyphosphoryl-5-methyl-1-pyrroline *N*-oxide  
298 superoxide adduct). According to these authors, the kinetic pattern of the radical adduct over time is the  
299 result of two different and independent processes: the formation and the decomposition of the adduct. In  
300 the formation process, the accumulation of the adduct over time depends on the number of radicals  
301 produced in the system and trapped by the spin trap if no other reactions quench the radical. In complex  
302 systems like oils, beer, wine, or plant extracts, it is likely that the endogenous antioxidants quench the  
303 radicals thus competing with the spin trap and slowing down the rate of adduct formation. The adducts  
304 have limited time stability, lower than the experiment duration, so once formed, the adducts decay  
305 relatively rapidly in no EPR detectable products.<sup>30</sup> For this reason, the concentration of the adduct  
306 measured in the kinetic curve is the result of a continuous equilibrium between formation and decay. On  
307 vegetable oils, the heat-induced radical formation is generally characterized by an initial slow adduct  
308 increase phase, whose length depends on oils, temperature, and the presence of antioxidants, followed by  
309 a sharp increase of the adduct signal.<sup>11, 16, 31</sup> The occurrence of the two phases is essential to calculate the IP  
310 (induction period), a parameter correlated to oils oxidative stability.<sup>4, 11, 32</sup>

311 Recently Jiang *et al.*<sup>11</sup> calculated IP fitting the experimental points with the Boltzmann function according to  
312 Barr *et al.*<sup>16</sup> Due to its shape, the Boltzmann sigmoidal equation fits the part of the kinetic that describes  
313 the formation of the adduct, but it is unable to describe the last part of the kinetic, which concerns its  
314 decomposition. Moreover, even in the first part, the Boltzmann sigmoid equation could not match the

315 experimental points since the intensities of the adducts constantly increase with time, while the asymptote  
316 of the Boltzmann sigmoid equation is parallel to the x axis. To overcome this problem, we propose a  
317 modification of the Boltzmann sigmoid equation. The modified Boltzmann sigmoid equation is described in  
318 the materials and methods section. The new parameter introduced in the equation is the rise, which  
319 considers the slope of the experimental points of the first part of the curve (Figure S4). The rise is not  
320 directly involved in the calculation of the IP but its introduction in the curve equation determines a  
321 modification of the parameters used to calculate it. As can be observed in Figure S4 and in Table 1, the  
322 better fitting of the experimental points corresponding to the slow adduct increase phase provided by the  
323 new equation resulted in significantly higher IP values. The parameters used for the fitting are reported in  
324 Table S2.

325 In previous papers dealing with the determination of the oxidative stability of oils, the kinetic of the PBN  
326 adduct was followed for a short period of time without reaching the point of maximum intensity<sup>11</sup>. In the  
327 present paper, for the first time, the kinetic was followed beyond the point of maximum intensity until the  
328 achievement of equilibrium. Similarly to DEPMPO-OOH adduct kinetic described by Roubaud *et al.*<sup>30</sup> and  
329 Samouilov *et al.*,<sup>29</sup> the last part of the kinetic describes the decomposition of the adduct. According to these  
330 authors, the decay of the spin adduct does not follow any particular decay law but depends on the  
331 experimental conditions of the reaction. In this paper, the differences observed between EVOO and SO  
332 might be due to the different oil compositions rather than to the experimental conditions since the same  
333 conditions were applied to both oils. The experimental points of the decomposition part of the kinetic were  
334 fitted with a reverse Boltzmann sigmoid equation, which is reported in the materials and methods section.  
335 Even in this case, a correction for the slope of the last points has been applied to the equation. These  
336 parameters were used to calculate the width of the kinetic curve and the final time that is analogous to the  
337 IP.

338  
339

#### 340 **Sunflower and olive oil kinetic parameters**

341 Table 1 reports the IP values calculated with the Boltzmann and the modified Boltzmann equations and the  
342 curve width and final time calculated from the fitting of the Boltzmann reverse equation for EVOO and SO.  
343 Both in EVOO and SO, the Boltzmann equation significantly underestimates the IP. As already highlighted,  
344 the introduction of the new parameter in the Boltzmann equation is not involved in calculating the IP, but it  
345 slightly modifies the parameters used to calculate it. The IP and the other parameters extracted from the  
346 PBN-adduct intensity curve vs. time were significantly different between SO and EVOO. As expected, the IP  
347 of EVOO is significantly higher than that of SO. Papadimitriou *et al.*<sup>32</sup> calculated the induction period (lag  
348 time) of some Greek olive oils and observed a strong correlation between the oxidative stability and the  
349 concentration of polyphenols, whereas no correlation was found with tocopherols. Our results agree with

350 the hypothesis of polyphenols' involvement in enhancing oils' oxidative stability since no phenolic  
351 compounds were detected in SO. At the same time, the different lag time of EVOO and SO may be the  
352 result of a different oxygen diffusivity into the oil since, as it will be discussed later, the induction period  
353 (i.e., lag time) was demonstrated to be indirectly proportional to the oxygen concentration in the oil.<sup>33</sup>  
354 Along with the lag time, even the curve width and the final time, calculated from the part of the kinetic  
355 related to the decomposition of the adduct, can discriminate between SO and EVOO.  
356 In the SO, the chain reactions occurring during lipid oxidation run out faster than in the EVOO, as  
357 demonstrated by the greater slope of the curve and the narrower curve width (Figure S5).  
358 A comparison of the slope of the two curves shows that with olive oil, the increase of the adduct signal  
359 intensity is slower than with sunflower oil, probably because polyphenolic compounds compete with PBN  
360 for the quenching/trapping of radical species. The lower maximum intensity value observed for olive oil  
361 could be explained in the same way. Therefore, the amount of antioxidants in oils affects the slope of the  
362 kinetic curve and the value of its intensity maximum. In sunflower oil, no phenolic compounds were  
363 detected, whereas olive oil was rich in secoiridoids and derivatives that are responsible for its high  
364 antioxidant properties.

365

366

#### 367 **Effect of the sample holder on the kinetic of PBN adduct in SO**

368 The presence of an IP and the shape of the kinetic curve depend on the conditions applied during the  
369 experiment. Temperature is one of the main experimental factors affecting it. On grape seed oil, Vicente *et*  
370 *al.*,<sup>14</sup> studying the effect of temperature on the formation and decomposition of PBN adduct, observed that  
371 the adduct half-life significantly decreased with increasing temperature, and at temperatures higher than  
372 180 °C, the stability of the adduct was too low to allow any time-course experiment. The same authors,  
373 plotting against time the EPR spectral intensities of oils heated at temperatures ranging from 105 to 180 °C,  
374 observed increasing rates of adduct formation with rising temperatures, suggesting the involvement of  
375 different oil-derived radicals in the reaction.<sup>14</sup> Similarly, Jiang *et al.*<sup>11</sup> studied the effect of temperature on  
376 PBN-adduct intensity during EPR experiments demonstrating that the higher the temperature, the greater  
377 the intensity of the adduct. In this paper, the choice of the temperature of 90 °C was based on preliminary  
378 results on oils and on other plant extracts;<sup>7</sup> agreeing with Jiang *et al.*,<sup>11</sup> who identified 90 °C as the best  
379 choice for IP determination in EPR experiments following the evolution over the time of the PBN adduct  
380 intensity. It is important to notice that the experiments cited above were performed heating the oil or the  
381 extracts in situ in the spectrometer cavity, while other experiments on olive or soybean oils were  
382 performed heating the oils outside the cavity, then measuring the adduct intensity at room temperature.<sup>4,9,</sup>

383 <sup>34</sup>

384 Even if the temperature can increase lipid oxidation rates, alone is not sufficient to affect oils' oxidative  
385 stability. According to several authors, oxygen is the main responsible for the oxidation process of edible  
386 oils,<sup>3,33</sup> in particular the amount of dissolved oxygen that can react with lipids and the oxygen reacting at oil  
387 surface are the main responsible for lipid oxidation.

388 Figure 2 shows the kinetic pattern of SO analyzed in three different sample holders and heated at 90 °C  
389 inside the EPR cavity. The IP is not easily identifiable in the flat cell as the adduct increases rapidly from the  
390 beginning of the experiment. By contrast, the adduct grows more slowly in capillary tubes: the narrower  
391 the capillary, the more slowly the adduct grows. The kinetic curves in Fig. 2 also differ for the maximum  
392 intensity of the adduct ( $I_{\max}$ ). However, the  $I_{\max}$  values obtained with the three sample holders cannot be  
393 directly compared since the volume of oil contained inside the EPR cavity decreases in the order: flat cell >  
394 large capillary tube > thin capillary tube, because of the different diameter of these sample holders (see  
395 Experimental).

396 The SO contained in flat cell had a significantly shorter IP than the same oil contained in capillary tubes  
397 (Table 2). As can be noticed in Table 2, the IP increased in the order: flat cell < large capillary tube < thin  
398 capillary tube. Besides the IP, the sample holder affected the time at which  $I_{\max}$  is reached: oils inside the  
399 flat cell reached it earlier than those in capillary tubes. At the same time, the shape of the sample tube  
400 affects the parameters that describe the decomposition of the adduct in the kinetic curve. The width of the  
401 curve of oil in thin capillary tubes was significantly larger than that in the other two sample tubes. Similarly,  
402 the "final time", which can be considered the opposite of the IP, was significantly higher in thin capillary  
403 tubes than in flat cells or large capillary tubes.

404 As explained above, oxygen has a critical role in free radical generation in heated lipids.<sup>15</sup> In degassed  
405 samples of linolenate, linoleate, and oleate heated at 105 °C, the shape of the spectral intensities over time  
406 were similar to those of aerated samples but with lower rates of generation and with lower spectral  
407 intensities.<sup>15</sup> Šimon *et al.*<sup>33</sup> observed that the length of the induction period was inversely proportional to  
408 the concentration of oxygen in the oil. According to these authors, oils' oxygen concentration depends on  
409 the equilibrium between oxygen amount that reacts with lipids and the one present in the headspace. At  
410 equilibrium, the oxygen concentration in the oil is determined by the diffusion coefficient, an oil  
411 characteristic, and the oils' surface (S) exposed to air. In the absence of mechanical agitation, diffusion is  
412 the only way for oxygen to be dissolved in oils. However, at temperatures higher than 60 °C, the oil oxygen  
413 concentration decreases as a consequence of the enhanced oxidation rates and the low oxygen solubility.  
414 Our experiments were carried out all at the same temperature (90 °C) and with the same oil volume (100  
415  $\mu\text{L}$ ), but the oil's surface exposed to oxygen was different among sample tubes. In the flat cell, oil had an  
416 exposed surface of 5  $\text{mm}^2$ , while in large and thin capillary tubes, it had a surface exposed to air of 1 and 2  
417  $\text{mm}^2$ ; thus, the oil to air interface seems the key point for the different curve shapes observed for the

418 heated oils. The greater the contact surface with the air, the greater the amount of oxygen reacting on the  
419 oil surface and the amount of adduct formed.

420

421 Figure 2

422

423 Table 2

424

#### 425 **Effect of oxygen availability on the formation of PBN adduct in SO**

426 To evaluate the effect of oxygen availability and oil surface exposed to air on peroxide value and on PBN  
427 adduct intensity, sunflower oil was heated at 90 °C for 15 h in 1.5 and 0.5 mL volume safe-lock sample  
428 tubes. In half of the sample tubes, the headspace volume was reduced to limit oxygen availability. In a  
429 recent paper, Velasco *et al.*<sup>12</sup> reported that low oxygen diffusion from the headspace of the EPR tube and  
430 the low surface-to-volume ratio contributed to limit oxidation. However, the temperature has a great effect  
431 on lipid oxidation rates and on oxygen solubility in bulk oils. For this reason, the results of this study cannot  
432 be directly compared with ours because they were obtained at 40 °C.

433 In SO heated at 90 °C with PBN, the headspace volume reduction had no effect either on peroxide values or  
434 on PBN adduct intensities measured by EPR. By contrast, in samples without PBN, SO in full volume tubes  
435 had significantly higher peroxide values than oil in reduced volume tubes (Figure 3A). Similar results were  
436 achieved when SO was heated with or without PBN in 0.5 mL safe-lock tubes (Figure 3C, 3D). In this case,  
437 however, in SO with PBN, some differences, albeit not significant, can be observed between full and  
438 reduced volume. The effect of oxygen availability is more clear observing the values of the adduct intensity:  
439 when the availability of oxygen is higher, the intensity of the adduct is significantly higher.

440 When PBN is present in the reaction mixture, it hinders the radicals' chain reaction by trapping lipid radicals  
441 and likely reduces the effect of oxygen on the oxidation process. There is competition between oxygen and  
442 PBN for the reaction with free radicals, which affects the extent of oxidation.

443 The reaction between radicals and PBN is favored over the reaction with oxygen because at the  
444 temperature of 90 °C oxygen solubility is rather low. This scenario changes when PBN is not present, so the  
445 reaction is controlled by oxygen availability only. As highlighted by Crapiste *et al.*<sup>35</sup> if oxygen supply is  
446 unlimited, oxidation rates depend on oil surface exposed to air and sample volume. In that paper, oil was  
447 heated at 47 °C, so the oil's surface exposed to air determined the amount of oxygen which dissolved in the  
448 oil volume. At higher temperatures (90 °C), as in our experiment, the oxygen solubility in oil is much lower,  
449 and the oxidation processes take place at the air/oil interface.

450 To evaluate the effect of the exposed surface on peroxide amount and on PBN adduct intensity, we paired  
451 off data of 1.5 mL sample tubes with those of 0.5 mL in both full volume and reduced volume. Under full  
452 oxygen availability conditions (full volume), no differences in peroxide value and EPR intensity were

453 observed between oils with a different exposed surface, neither with PBN nor without (supplementary  
454 materials Figure S6A, S6B). Conversely, Crapiste *et al.*<sup>35</sup> observed, in SO stored at 47 °C for 60 days, an  
455 enhancement of peroxide values with increasing S/V ratios.

456 In our experiments, when oxygen availability was reduced (reduced volume), the oils with a higher exposed  
457 surface (1.5 mL sample tubes) had significantly higher PBN adduct signal intensity. When there are no  
458 restrictions on oxygen availability, the concentration of dissolved oxygen in bulk oil is lower than the  
459 amount available in the headspace because, at 90 °C, its solubility is low.

460 On the contrary, when oxygen availability is limited, oxygen solubility in oil is likely higher than its  
461 availability in the headspace, so the exposed surface regulates oxygen uptake: the lower the exposed  
462 surface, the lower is the amount of oxygen reacting with lipids. Thus the PBN adduct signal intensity  
463 decreases.

464

465 Figure 3

466

467

#### 468 **Peroxides, conjugated dienes and PBN-adduct intensity of SO and EVOO treated at 90 °C**

469 To understand what was happening during the thermal treatment at 90 °C, we simultaneously measured  
470 the peroxide value, the adduct's EPR intensity, and the conjugated dienes and trienes of SO and EVOO at  
471 different time intervals during a time-course experiment (Figure 4). The EPR spectra were obtained  
472 collecting 100 µL of oil containing PBN, kept at 90 °C in 1.5 mL Eppendorf safe-lock tubes for the desired  
473 time interval; on the same samples, PV and conjugated dienes and trienes were also measured (Figure 4).  
474 Peroxide values, dienes, and trienes were also measured in samples subjected to the same thermal  
475 treatment but without the addition of PBN. While designing the experiment, the choice of the time  
476 intervals for the analysis was based on the kinetic curve of the PBN adduct measured in the flat cell heated  
477 at 90 °C into the EPR cavity. In particular, the points corresponding approximately to the IP, the  $V_{50}$ , the  
478  $I_{max}$ , and the point of equilibrium in the final part of the kinetic curve have been chosen. However, as shown  
479 in Figure 4, the reaction time in 1.5 mL safe-lock tubes is much longer than that measured in the flat cell or  
480 in the capillary tubes. For this reason, we decided to continue with the thermal treatment beyond 5 hours,  
481 the time at which the kinetic EPR experiment was ended. Results show that even after 1800 min (30 hours),  
482 the maximum of the EPR intensity was not reached, while in the flat cell, the maximum was at *ca.* 106 min.  
483 This further confirms the importance of the sample holder and the oil exposed surface to air during the oil  
484 thermal treatment.

485 As pointed out by some authors,<sup>4, 34</sup> the use of spin trapping agents like PBN during oil accelerated ageing  
486 interferes with the free radical mechanism of oxidation since, once trapped by PBN, the free radical species  
487 cannot propagate the chain mechanism inhibiting the oxidation process.

488

489 Figure 4

490

491 This is clear comparing the peroxide values measured in sunflower and olive oils with and without PBN. The  
492 presence of PBN significantly decreased the peroxide values from the beginning of the experiment, but its  
493 effect grew over time. The inhibiting effect of PBN was observed in SO, rapeseed, and fish oils heated at 40  
494 °C by Velasco *et al.*<sup>34</sup> According to these authors, the extent of PBN inhibition was dependent on the type of  
495 oil. In particular, they observed that the effect of PBN on lipid oxidation was related to oils' oxidative  
496 stability: the lower the oxidative stability, the larger the effect of PBN on oxidation rate. Even at 90 °C, PBN  
497 shows an inhibiting effect. Moreover, our results on EVOO confirm the differences among oils. Up to 6  
498 hours of heating treatment at 90 °C, in EVOO, no differences could be detected between samples with and  
499 without PBN. By contrast, in SO PBN inhibited lipid oxidation from the beginning of the experiment.

500 Velasco *et al.*<sup>34</sup> ascribed the extent of the PBN inhibiting effect to the presence of tocopherols, showing  
501 that the PBN inhibiting effect of lipid oxidation was higher in oils with low amounts of tocopherols in  
502 comparison with the added PBN. In the literature is reported that the amount of tocopherols in SO is nearly  
503 four-fold higher than in olive oil.<sup>36</sup> For this reason, we should expect a higher PBN's inhibiting effect in  
504 EVOO. It is evident from Figure 4A and 4C that the PBN inhibiting effect is higher in SO because in this oil is  
505 larger the difference in PV values in samples with and without PBN, while the EPR intensity in SO is higher  
506 than in EVOO (the higher the PBN inhibiting effect, the higher is the intensity of the EPR signals of the PBN  
507 adducts). Tocopherols alone do not explain the inhibiting effects of PBN observed on SO and EVOO.  
508 Therefore, other polyphenolic compounds, of which EVOO is rich (see Table S1), compete with PBN and  
509 decrease its inhibiting effect of lipid oxidation.

510 To understand whether the PBN concentration might increase the PBN inhibiting effect of lipid oxidation,  
511 peroxide values were measured in sunflower oil containing PBN at different concentrations and heated at  
512 90 °C for 5 hours (Figure S7). The results indicate that PBN concentration had no effect on peroxide value,  
513 at least in the range of concentrations (62.5 – 250 mM) examined here.

514 The evolution of the conjugated dienes confirmed the peroxide values obtained for sunflower and olive oils  
515 (figure 4B and 4D). Conjugated trienes were not affected by either thermal treatment or PBN (data not  
516 shown). The values of conjugated dienes are an index of secondary products of lipid oxidation. Their levels  
517 are associated with the oxidative stability of the oils: high levels of dienes reflect low oxidative stability, as  
518 confirmed in this work, in which EVOO had the lowest values. In the present study, conjugated dienes of SO  
519 and EVOO increased during the thermal treatment. The presence of PBN diminished the values of  
520 conjugated dienes with a different extent of depletion between oils.



521 In this paper, for the first time, an analysis of the kinetic curve of the PBN adduct was performed. When  
522 sunflower and virgin olive oil are heated at 90 °C in the presence of PBN, the generated radical species  
523 could react with the antioxidants or be trapped by spin trapping molecules (PBN or DMPO) originating  
524 relatively stable radical species, which can be easily detected by EPR. The kinetic curves representing the  
525 EPR intensity of the PBN adducts vs. time can be divided in two parts considering the formation of the  
526 adduct and its decomposition. Both adduct formation and decomposition were fitted with two modified  
527 Boltzmann sigmoidal equations.

528 The new equation, proposed here for the first time, allows obtaining a more realistic value of the lag time  
529 (or final time) because the asymptotes of the Boltzmann sigmoidal equation are not perfectly horizontal,  
530 but slightly “rise”. The lag time, the curve width and the final time, calculated from the fitting parameters  
531 allow for distinguishing SO from EVOO.

532 The experimental conditions affecting the kinetic analysis of the PBN adduct were also studied. In this  
533 paper it was demonstrated that the same oil heated in different sample holders produce kinetic curves of  
534 different shape, thus affecting the parameters proposed to discriminate oils. This aspect should be carefully  
535 taken into account when comparing results from different laboratories. In experiments performed at 90 °C,  
536 where the oxygen solubility is low, a key factor which influences the experimental results is the oil surface  
537 exposed to air. In these conditions the reactions with oxygen take place at the oil/air interface and not in  
538 the bulk oil where the oxygen solubility is limited. The results obtained in this work allow for reaching a  
539 better knowledge of the factors which influence thermal treatment coupled with spin trapping  
540 experiments. The proposed Boltzmann modified sigmoidal equation can be applied to other fields, like the  
541 study of lag time of beers, exploring the whole kinetic curve and not only the first part, which allows for  
542 determining the lag time value.

543

544

## 545 REFERENCES

- 546 1. Andersen, M. L.; Skibsted, L. H. In *Antioxidant Measurement and Applications*; Shahidi, F., Ho, C. T.,  
547 Ed.; 2007; Vol. 956, pp 106-117.
- 548 2. Choe, E.; Min, D. B. Mechanisms and Factors for Edible Oil Oxidation. *Comp. Rev. Food Sci. Food*  
549 *Safety* **2006**, 5 (4), 169-186.
- 550 3. Johnson, D. R.; Decker, E. A. The Role of Oxygen in Lipid Oxidation Reactions: A Review. *Annu. Rev.*  
551 *Food Sci. Technol.* **2015**, 6 (1), 171-190.
- 552 4. Cui, L.; Lahti, P. M.; Decker, E. A. Evaluating Electron Paramagnetic Resonance (EPR) to Measure  
553 Lipid Oxidation Lag Phase for Shelf-Life Determination of Oils. *J. Am. Oil Chem. Soc.* **2017**, 94 (1), 89-97.

- 554 5. Merkx, D. W. H.; Plankensteiner, L.; Yu, Y.; Wierenga, P. A.; Hennebelle, M.; Van Duynhoven, J. P. M.  
555 Evaluation of PBN spin-trapped radicals as early markers of lipid oxidation in mayonnaise. *Food Chem.*  
556 **2021**, 334, 127578.
- 557 6. Ricca, M.; Fodera, V.; Vetri, V.; Buscarino, G.; Montalbano, M.; Leone, M. Oxidation Processes in  
558 Sicilian Olive Oils Investigated by a Combination of Optical and EPR Spectroscopy. *J. Food Sci.* **2012**, 77 (10),  
559 C1084-C1089.
- 560 7. Sanna, D.; Mulas, M.; Molinu, M. G.; Fadda, A. Oxidative stability of plant hydroalcoholic extracts  
561 assessed by EPR spin trapping under forced ageing conditions: A myrtle case study. *Food Chem.* **2019**, 271,  
562 753-761.
- 563 8. Ottaviani, M. F.; Spallaci, M.; Cangiotti, M.; Bacchiocca, M.; Ninfali, P. Electron paramagnetic  
564 resonance investigations of free radicals in extra virgin olive oils. *J. Agric. Food Chem.* **2001**, 49 (8), 3691-  
565 3696.
- 566 9. Velasco, J. n.; Andersen, M. L.; Skibsted, L. H. Evaluation of oxidative stability of vegetable oils by  
567 monitoring the tendency to radical formation. A comparison of electron spin resonance spectroscopy with  
568 the Rancimat method and differential scanning calorimetry. *Food Chem.* **2004**, 85 (4), 623-632.
- 569 10. Papadimitriou, V.; Maridakis, G. A.; Sotiroudis, T. G.; Xenakis, A. Antioxidant activity of polar  
570 extracts from olive oil and olive mill wastewaters: an EPR and photometric study. *Eur. J. Lipid Sci. Technol.*  
571 **2005**, 107 (7-8), 513-520.
- 572 11. Jiang, S.; Xie, Y.; Li, M.; Guo, Y.; Cheng, Y.; Qian, H.; Yao, W. Evaluation on the oxidative stability of  
573 edible oil by electron spin resonance spectroscopy. *Food Chem.* **2020**, 309, 125714.
- 574 12. Velasco, J.; Andersen, M. L.; Skibsted, L. H. ESR spin trapping for in situ detection of radicals  
575 involved in the early stages of lipid oxidation of dried microencapsulated oils. *Food Chem.* **2021**, 341,  
576 128227.
- 577 13. Silvagni, A.; Franco, L.; Bagno, A.; Rastrelli, F. Thermoinduced Lipid Oxidation of a Culinary Oil: A  
578 Kinetic Study of the Oxidation Products by Magnetic Resonance Spectroscopies. *J. Phys. Chem. A* **2010**, 114  
579 (37), 10059-10065.
- 580 14. Vicente, L.; Deighton, N.; Glidewell, S. M.; Empis, J. A.; Goodman, B. A. In situ measurement of free  
581 radical formation during the thermal decomposition of grape seed oil using "spin trapping" and electron  
582 paramagnetic resonance spectroscopy. *Z. Lebensm. Unters. Forsch.* **1995**, 200 (1), 44-46.
- 583 15. Vicente, L. M.; Empis, J. A.; Deighton, N.; Glidewell, S. M.; Goodman, B. A.; Rowlands, C. C. Use of  
584 EPR and ENDOR spectroscopy in conjunction with the spin trapping technique to study the high-  
585 temperature oxidative degradation of fatty acid methyl esters. *J. Chem. Soc., Perkin Trans. 2* **1998**, (2), 449-  
586 454.
- 587 16. Barr, D.; Reynhout, G.; Guzinski, J. *Measuring Oxidation of Cooking oil using EPR Spin Trapping.*  
588 Bruker BioSpin 12/09 T118662.

- 589 17. Xie, Y.; Jiang, S.; Li, M.; Guo, Y.; Cheng, Y.; Qian, H.; Yao, W. Evaluation on the formation of lipid free  
590 radicals in the oxidation process of peanut oil. *LWT* **2019**, 104, 24-29.
- 591 18. Deiana, P.; Santona, M.; Dettori, S.; Culeddu, N.; Dore, A.; Molinu, M. G. Multivariate approach to  
592 assess the chemical composition of Italian virgin olive oils as a function of variety and harvest period. *Food*  
593 *Chem.* **2019**, 300, 125243.
- 594 19. Shantha, N. C.; Decker, E. A. Rapid, Sensitive, Iron-Based Spectrophotometric Methods for  
595 Determination of Peroxide Values of Food Lipids. *J. AOAC Int.* **1994**, 77 (2), 421-424.
- 596 20. SPECTROPHOTOMETRIC INVESTIGATION IN THE ULTRAVIOLET. In *COI/T.20/Doc. No 19/Rev. 5*,  
597 INTERNATIONAL OLIVE COUNCIL: 2019.
- 598 21. Papanikolaou, C.; Melliou, E.; Magiatis, P. In *Functional foods*; Lagouri, V., Ed.; IntechOpen: 2018.
- 599 22. Andersen, M. L.; Skibsted, L. H. Electron Spin Resonance Spin Trapping Identification of Radicals  
600 Formed during Aerobic Forced Aging of Beer. *J. Agric. Food Chem.* **1998**, 46 (4), 1272-1275.
- 601 23. Andersen, M. L.; Skibsted, L. H. In *Modern Magnetic Resonance*; Webb, G. A., Ed.; Springer  
602 Netherlands: Dordrecht, 2006; pp 1861-1866.
- 603 24. Nikolantonaki, M.; Coelho, C.; Noret, L.; Zerbib, M.; Vileno, B.; Champion, D.; Gougeon, R. D.  
604 Measurement of white wines resistance against oxidation by Electron Paramagnetic Resonance  
605 spectroscopy. *Food Chem.* **2019**, 270, 156-161.
- 606 25. Alberti, A.; Macciantelli, D. In *Electron Paramagnetic Resonance: A Practitioner's Toolkit*; Brustolon,  
607 M., Giamello, E., Ed.; John Wiley & Sons, Inc.: Hoboken, New Jersey, 2009; Chapter 8, pp 287-323.
- 608 26. Yamada, T.; Niki, E.; Yokoi, S.; Tsuchiya, J.; Yamamoto, Y.; Kamiya, Y. Oxidation of lipids. XI. Spin  
609 trapping and identification of peroxy and alkoxy radicals of methyl linoleate. *Chem. Phys. Lipids* **1984**, 36  
610 (2), 189-196.
- 611 27. Chen, H. J.; Wang, Y.; Cao, P. R.; Liu, Y. F. Thermal Oxidation Rate of Oleic Acid Increased  
612 Dramatically at 140 degrees C Studied using Electron Spin Resonance and GC-MS/MS. *J. Am. Oil Chem. Soc.*  
613 **2019**, 96 (8), 937-944.
- 614 28. Caglar, M. U.; Teufel, A. I.; Wilke, C. O. Sicegar: R package for sigmoidal and double-sigmoidal curve  
615 fitting. *PeerJ* **2018**, 6, e4251.
- 616 29. Samouilov, A.; Roubaud, V.; Kuppusamy, P.; Zweier, J. L. Kinetic analysis-based quantitation of free  
617 radical generation in EPR spin trapping. *Anal. Biochem.* **2004**, 334 (1), 145-154.
- 618 30. Roubaud, V.; Sankarapandi, S.; Kuppusamy, P.; Tordo, P.; Zweier, J. L. Quantitative Measurement of  
619 Superoxide Generation Using the Spin Trap 5-(Diethoxyphosphoryl)-5-methyl- 1-pyrroline-N-oxide. *Anal.*  
620 *Biochem.* **1997**, 247 (2), 404-411.
- 621 31. Chen, H.; Cao, P.; Li, B.; Sun, D.; Li, J.; Liu, Y. High sensitive and efficient detection of edible oils  
622 adulterated with used frying oil by electron spin resonance. *Food Control* **2017**, 73, 540-545.

- 623 32. Papadimitriou, V.; Sotiroudis, T. G.; Xenakis, A.; Sofikiti, N.; Stavyiannoudaki, V.; Chaniotakis, N. A.  
624 Oxidative stability and radical scavenging activity of extra virgin olive oils: An electron paramagnetic  
625 resonance spectroscopy study. *Anal. Chim. Acta* **2006**, 573–574, 453-458.
- 626 33. Šimon, P.; Kolman, L.; Niklová, I.; Schmidt, Š. Analysis of the induction period of oxidation of edible  
627 oils by differential scanning calorimetry. *J. Am. Oil Chem. Soc.* **2000**, 77 (6), 639-642.
- 628 34. Velasco, J.; Andersen, M. L.; Skibsted, L. H. Electron Spin Resonance Spin Trapping for Analysis of  
629 Lipid Oxidation in Oils: Inhibiting Effect of the Spin Trap  $\alpha$ -Phenyl-N-tert-butyl nitron on Lipid Oxidation. *J.*  
630 *Agric. Food Chem.* **2005**, 53 (5), 1328-1336.
- 631 35. Crapiste, G. H.; Brevedan, M. I. V.; Carelli, A. A. Oxidation of sunflower oil during storage. *J. Am. Oil*  
632 *Chem. Soc.* **1999**, 76 (12), 1437.
- 633 36. Wagner, K. H.; Kamal-Eldin, A.; Elmadfa, I. Gamma-Tocopherol – An Underestimated Vitamin? *Ann.*  
634 *Nutr. Metab.* **2004**, 48 (3), 169-188.

635

636

637

638

639 Figure captions

640

641 Figure 1. A: EPR spectra measured at a) 36 min; b) 106 min and c) 146 min during the thermal treatment of  
642 sunflower oil at 90 °C in the presence of PBN in the flat cell; B: Experimental and simulated EPR spectra of  
643 sunflower oil containing DMPO obtained during thermal treatment at 90 °C. a) experimental (full line) and  
644 simulated (dotted line) spectrum at 11 min; b) experimental (full line) and simulated spectra (dotted lines)  
645 at 81 min. Asterisks indicate minor adducts present at the beginning of the experiment.

646

647 Figure 2. Kinetic curves of sunflower oil heated with PBN (125 mM final concentration) at 90 °C and placed  
648 in a flat cell (●), large capillary tubes (○) and thin capillary tubes (▲).

649

650 Figure 3. Peroxide values and PBN adduct intensity of sunflower oil heated for 15 h at 90 °C in safe-lock  
651 sample tubes of 1.5 (A and B) and 0.5 mL (C and D). White bars indicate tubes where internal volume has  
652 been reduced, while black bars indicate tubes without any volume reduction. Bars with different letters are  
653 statistically different according to Tukey's test ( $P \leq 0.05$ ).

654

655 Figure 4. Evolution of peroxide value (A and C, fuchsia and black lines), EPR intensity (PBN adduct signal  
656 intensity (AU)) (A and C, purple line) and conjugated dienes (B and D) during the time course of thermal  
657 treatment of sunflower oil (A and B) and Olive oil (C and D) at 363 K in 1.5 mL safe-lock sample tubes. In all  
658 graphs fuchsia lines indicate oil samples without PBN whereas black lines indicate oil samples with the  
659 addition of PBN.

660

661

662

663

664

665

666

667

Table 1. Kinetic parameters calculated from the kinetic curves of sunflower and olive oil heated with PBN (125 mM final concentration) at 90 °C in flat cell.

Kinetic parameters												
Adduct formation						Adduct decomposition						
Oils	IP				Slope				Curve width		Final time	
	Boltzmann		Boltzmann modified		Boltzmann		Boltzmann modified					
Olive	47.71 ± 4.7	bA	60.36 ± 5.2	aA	37.74 ± 6.1	aA	32.10 ± 5.1	aA	101.63 ± 3.8	A	228.6 ± 13.3	A
Sunflower	22.63 ± 3.5	bB	35.92 ± 2.7	aB	26.43 ± 2.6	aB	18.68 ± 2.9	bB	72.64 ± 4.5	B	144.00 ± 0.1	B

Data are presented as mean ± SD. Capital letters relate to differences between oils while lower case letters relate to differences between lag times calculated with Boltzmann and modified Boltzmann equations within the same oil. Differences were calculated according to Student's *t*-test ( $P \leq 0.05$ ).

1 Table 2. Parameters extracted from the kinetic curves of sunflower oil heated at 90 °C and  
2 placed in different sample tubes.

<b>Sample tubes</b>	<b>IP (min)</b>	<b>curve width (Mid<sub>2</sub> - V<sub>50</sub>)</b>	<b>Final time (min)</b>
Flat cell	35.92 ± 2.7 <b>c</b>	72.64 ± 4.5 <b>b</b>	144.00 ± 0.1 <b>b</b>
Large capillary tubes	47.08 ± 5.2 <b>b</b>	78.18 ± 2.4 <b>ab</b>	181.77 ± 16.2 <b>b</b>
Thin capillary tubes	69.54 ± 0.3 <b>a</b>	89.10 ± 0.1 <b>a</b>	231.08 ± 1.7 <b>a</b>

3 Each value is the mean of three replicates ± standard deviation. Means with different letters within the same column are statistically different by  
4 Tukey's test (P ≤ 0.05).

5

6

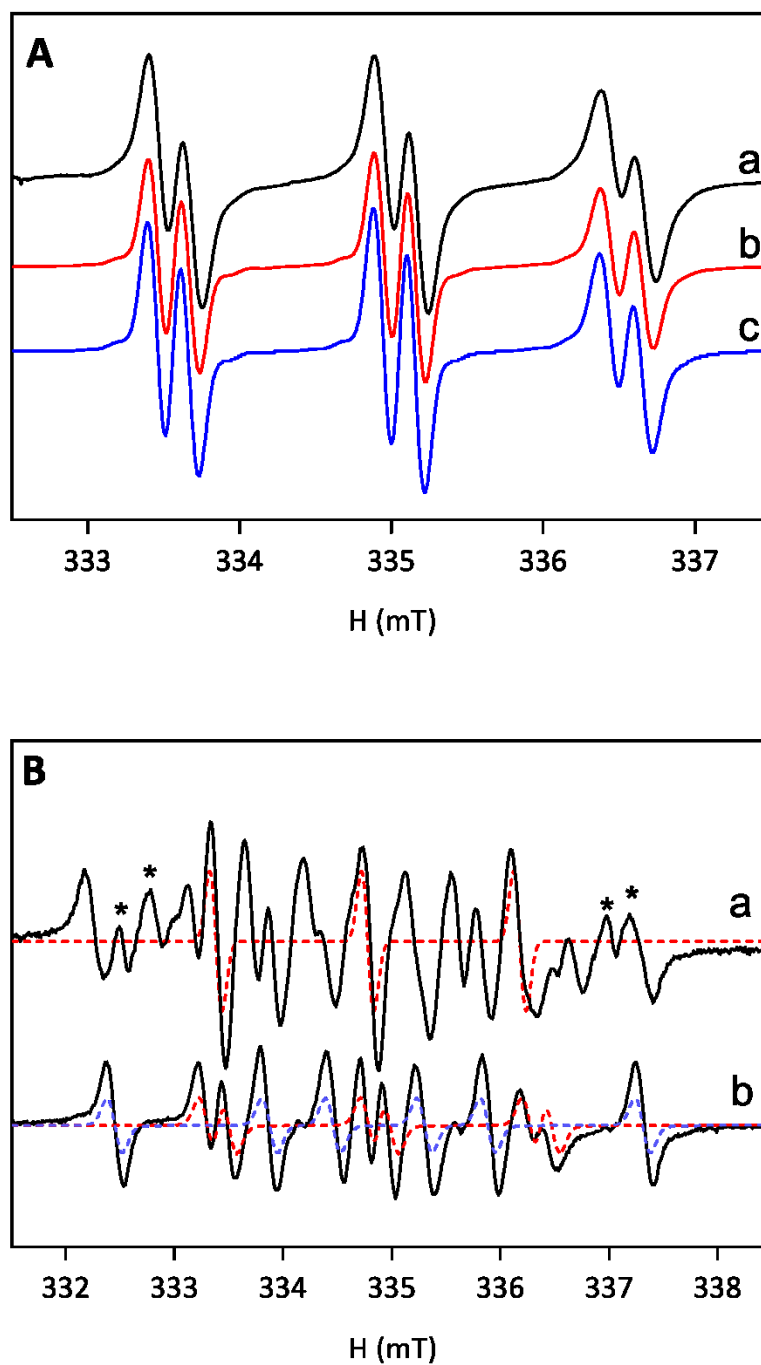
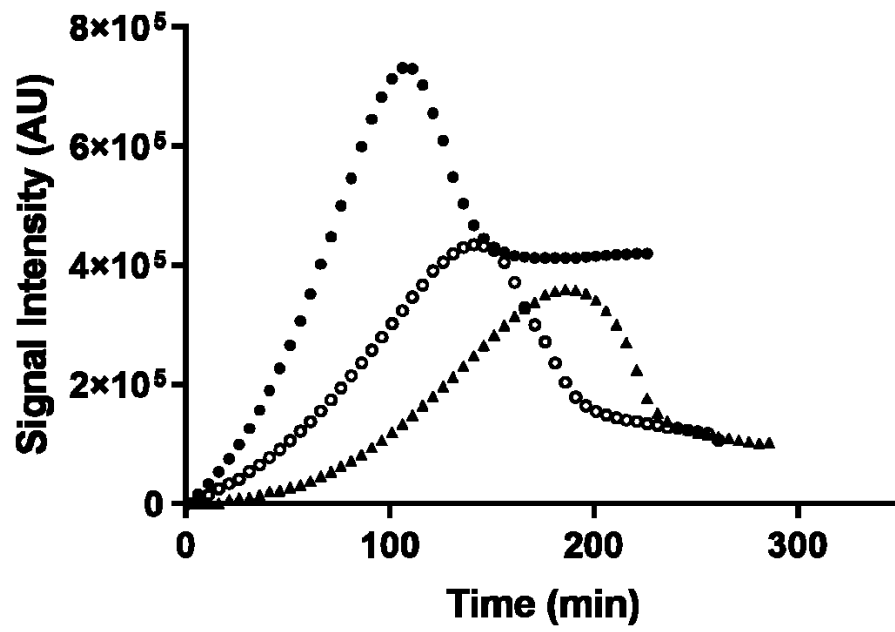


Figure 1. A: EPR spectra measured at a) 36 min; b) 106 min and c) 146 min during the thermal treatment of sunflower oil at 90 °C in the presence of PBN in the flat cell; B: Experimental and simulated EPR spectra of sunflower oil containing DMPO obtained during thermal treatment at 90 °C. a) experimental (full line) and simulated (dotted line) spectrum at 11 min; b) experimental (full line) and simulated spectra (dotted lines) at 81 min. Asterisks indicate minor adducts present at the beginning of the experiment.





1

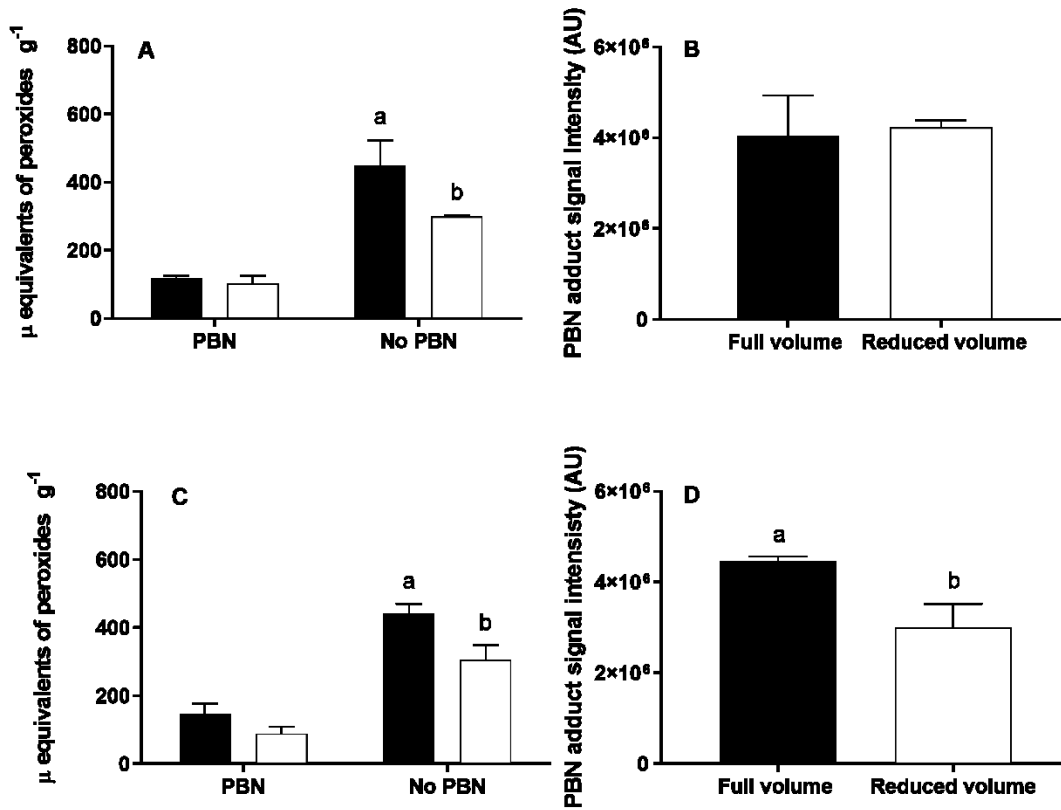
2

3 Figure 2. Kinetic curves of sunflower oil heated with PBN (125 mM final concentration) at 90 °C and placed  
4 in a flat cell (•), large capillary tubes (○) and thin capillary tubes (▲).

5

6

7



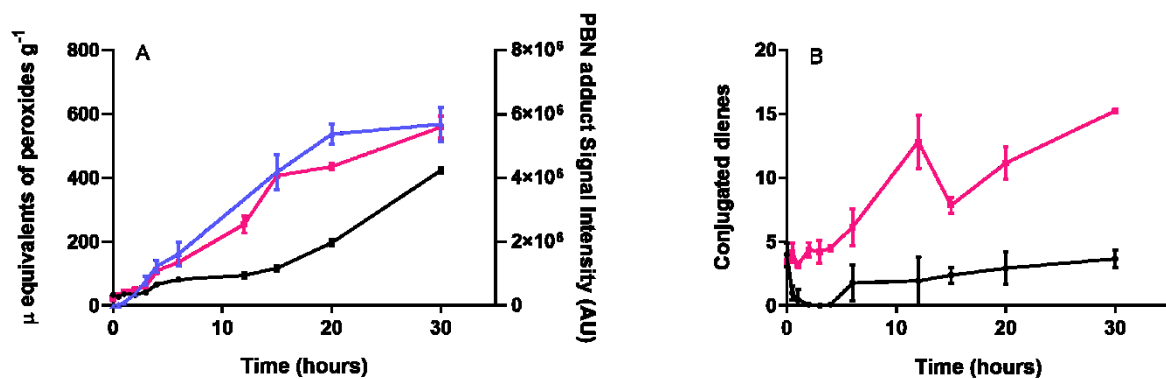
8

9 Figure 3. Peroxide values and PBN adduct intensity of sunflower oil heated for 15 h at 90 °C in safe-lock  
10 sample tubes of 1.5 (A and B) and 0.5 mL (C and D). White bars indicate tubes where internal volume has  
11 been reduced, while black bars indicate tubes without any volume reduction. Bars with different letters are  
12 statistically different according to Tukey's test ( $P \leq 0.05$ ).

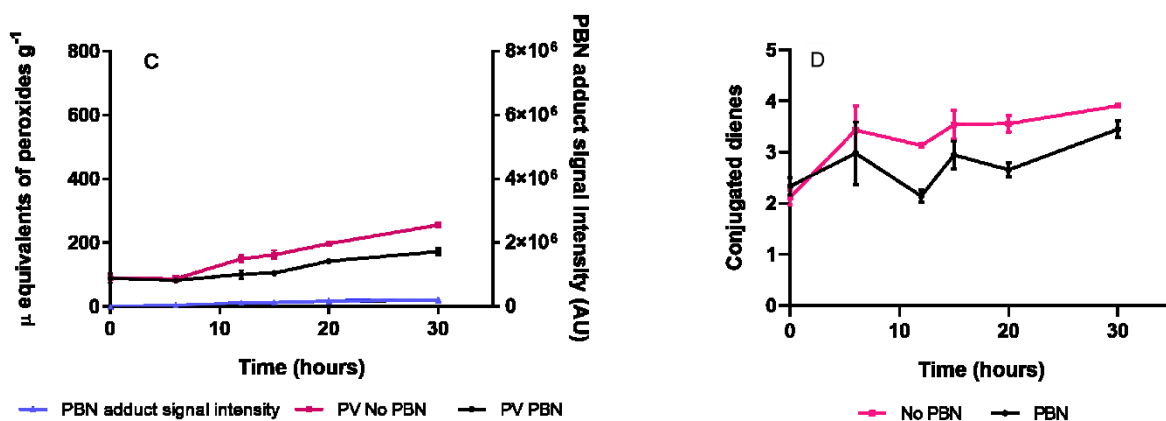
13

14

### Sunflower oil



### Extra virgin olive oil



15

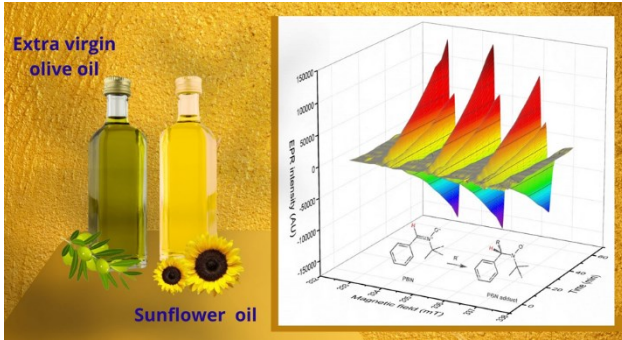
16 Figure 4. Evolution of peroxide value (A and C, fuchsia and black lines), EPR intensity (PBN adduct signal  
 17 intensity (AU)) (A and C, purple line) and conjugated dienes (B and D) during the time course of thermal  
 18 treatment of sunflower oil (A and B) and Olive oil (C and D) at 363 K in 1.5 mL safe-lock sample tubes. In all  
 19 graphs fuchsia lines indicate oil samples without PBN whereas black lines indicate oil samples with the  
 20 addition of PBN.

21

22

23 For Table of Contents Only

24



25

26

27